FEATURE ARTICLE

Understanding the Energy Transfer Function of LHCII, the Major Light-Harvesting Complex of Green Plants†

Herbert van Amerongen* and Rienk van Grondelle

Faculty of Sciences, Division of Physics and Astronomy, Department of Biophysics and Physics of Complex Systems, Vrije Universiteit Amsterdam, De Boelelaan 1081, 1081 HV Amsterdam, The Netherlands

Received: August 4, 2000; In Final Form: October 12, 2000

Since the crystal structure of the major light-harvesting complex II (LHCII) of green plants was obtained by Kühlbrandt, Wang and Fujiyoshi (*Nature* **199**4, *367*, 614−621), this chlorophyll-containing trimeric membrane protein has been the subject of intensive investigation. The complex contains between 36 and 42 chlorophyll molecules per trimer (Chl *a* and Chl *b*) and 10 to 12 xanthophyll molecules (lutein, neoxanthin and violaxanthin). The protein displays a rich spectrum of interactions, both between pigments and between the pigments and the protein, and these interactions have been studied with a multitude of different techniques. In this article we present an overview of the most important experimental results that have become available over the past decade and relate these to the structural knowledge. Emphasis will be put on the pigment identities, their spectroscopic features, and the interactions between the pigments, which determine both steady-state (polarized) properties and singlet and triplet energy transfer dynamics. Remaining questions will be pinpointed and hopefully they can help direct research in the near future.

Introduction

Photosynthesis in green plants takes place in Photosystems I and II (PSI and PSII), which are both conglomerates of a large number of proteins, many of which are responsible for pigment binding. PSI and PSII comprise hundreds of pigments, only a few of which are involved in charge separation, the crucial process that finally leads to the chemical storage of free energy.[1,2] Most of the pigments are involved in light harvesting, i.e., the absorption of sunlight and the transportion of electronic excitation energy toward the so-called reaction centers of PSI and PSII, where the charge separation takes place. The majority of the pigments in PSII of green plants are bound to the major peripheral antenna complexes, called LHCII. The basic unit of LHCII is trimeric; on average four of such trimeric LHCII's are present per PSII reaction center.[3] Recently, three different binding locations were identified in PSII complexes with the use of electron microscopy, and the binding affinities appeared to differ significantly.[4,5] A schematic representation of the different locations of LHCII is given in Figure 1. In addition, many PSII−LHCII supercomplexes in one membrane face only LHCII in another membrane in the so-called grana, which consist of stacked thylakoid membranes.[6] A possible existence of LHCII-only domains in the thylakoid membranes was corroborated by the structural characterization of a supramolecular complex consisting of seven trimeric LHCII complexes.[7] Figure 1 also shows the location of the minor peripheral antenna complexes CP24, CP26, CP29. These pigment−protein complexes show significant sequence homology with LHCII and

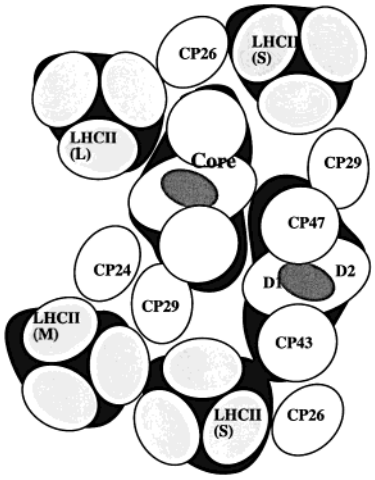

Figure 1. Schematic representation of part of the thylakoid membrane, containing PSII. Charge separation takes place in D1D2, which together with CP47 and CP43 forms the core. The minor Chl *a/b* proteins CP24, CP26 and CP29 are bound next to the core. LCHII can bind at different positions (S, indicating strong binding; M, moderately stong binding; L, loose binding). In the thylakoid membranes the stoichiometry of the different protein complexes is approximately: 1 core:1 CP24:1 CP26:1 CP29:4 trimeric LHCII. This indicates that LHCII also binds at additional locations.

* Corresponding author. Tel.: +31-20-4447931. Fax: +31-20-4447999. E-mail: herbert@nat.vu.nl.

† Abbreviations: Car, carotenoid; CD, circular dichroism; Chl *a*, chlorophyll *a*; Chl *b*, chlorophyll *b*; Chls, chlorophylls; DADS, decay associated difference spectra; fwhm, full width at half-maximum; LD, linear dichroism; LHCII, light-harvesting complex II of green plants; Lut, lutein; *n*, refractive index; Neo, neoxanthin; OD, optical density; PSI, Photosystem I.; PSII, Photosystem II.; PW, phonon wing; RT, room temperature; T−S, triplet-minus-singlet; Vio, violaxanthin; WT, wildtype; Xan, xanthophyll; Zea, zeaxanthin; ZPL, zero-phonon line.

10.1021/jp0028406 CCC: $20.00
Published on Web 12/23/2000

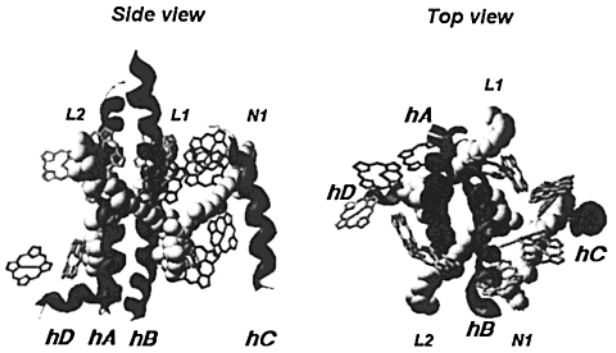

Figure 2. Molecular model of LHCII presented by Croce et al.[12] It is based on the crystal structure of Kühlbrandt et al.[11] and shows in addition the proposed location[12] of the neoxanthin molecule (N1). In the case of the side view, the viewer is "sitting" in the membrane, the top view looks onto the membrane. L1 and L2 represent the luteins. Helices A, B, C and D are represented by hA, hB, hC and hD, respectively. The figure was made by Giuseppe Insana, and kindly provided by Croce and Bassi and published in a somewhat different representation by Croce et al.[12]

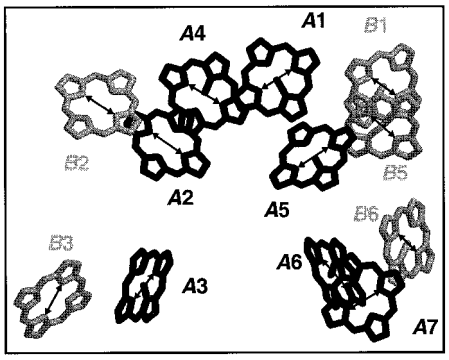

Figure 3. Tetrapyrrole rings that serve as model structures for chlorophyll in LHCII as determined by Kühlbrandt et al.[11] The double-headed arrows represent the "0" directions (see text). The numbering of the binding sites (capitals) is analogous to the numbering of the Chls in the original paper of Kühlbrandt et al.[11] (small letters with numbers). Note that for the model calculations in the present paper the Chl at site B1 was taken to be a Chl *a* and the Chl at site A6 was a Chl *b* molecule. All other chloropylls had the same identity as originally proposed.[11] For the model calculations all transition dipole moments were taken along the "0" direction except for the Chl at position B3, where it is along the "1" direction and is perpendicular to the "0" direction in the plane of the tetrapyrrole ring.

are generally believed to adopt a structure, similar to that of LHCII, although these minor complexes are monomeric.

In vitro, LHCII can aggregate in different ways:[8] (1) regular lamellar sheets, which are mainly two-dimensional in shape, (2) well organized three-dimensional structures, and (3) disordered three-dimensional structures. The trimeric pigment−protein complex is not unique in its composition and consists of various combinations of three very similar proteins, encoded by genes Lhcb1, Lhcb2 and Lhcb3, and they occur in a ratio of about 8: 3: 1.[3] The Lhcb1 and Lhcb2 gene products have only 14 differences in their amino acid sequences.[3] The Lhcb3 product is not only somewhat smaller (it lacks a number of amino acids at the N-terminus), but its amino acid sequence deviates on a variety of positions from those of the other two proteins. Except for the Lhcb3 gene product, LHCII contains a phosphorylation site and phosphorylation of this site is believed to cause "lateral" movement of LHCII between the granal and lamellar parts of the thylakoid membranes.[9] Therefore, LHCII has significant organizational flexibility, both in vivo and in vitro, which is accompanied by changes in optical properties, and which may have a regulatory function, for instance, in the flow of energy but also in the dissipation of excess excitations in bright sunlight (nonphotochemical quenching) (see, e.g., Ruban et al.[10]). It is our opinion that a thorough understanding of these properties and their variability first requires a detailed understanding of the organization and spectroscopy of trimeric and monomeric LHCII.

A major step forward in the understanding of light harvesting in PSII was the elucidation of the structure of LHCII by Kühlbrandt and co-workers,[11] combining results from electron diffraction and electron microscopy on two-dimensional crystals of LHCII at cryogenic temperatures and thereby it is one of the few structures of membrane proteins that is available to date. The resolution of the structure was 3.4 Å parallel to the plane of the trimer (which is also the plane of the 2-D crystals and the plane of the membrane), and 4.4−4.9 Å perpendicular to this plane. This resolution led to a somewhat crude model of the structure.[11] In Figure 2 a model of the LHCII monomeric subunit is shown that is based on the crystal structure, but in which an additional neoxanthin is put, based on the results of Croce et al.[12] The model shows large parts of the protein backbone as well as the locations and approximate orientations of 12 chlorophylls and two carotenoids. Particularly well-resolved are the three transmembrane α-helices (hA, hB and hC) and a short amphiphilic helix (hD) at the interface of the protein and the water surroundings. Helices A and B are exceptionally long, make an angle of about 30° with the normal to the membrane plane, and are held together by a pair of interhelix ionpairs. Helix C is shorter and is oriented parallel to the normal. The structure of a considerable part of the protein, in particular most of the connecting parts between the helices, as well as the C- and N-termini was not resolved. Noteworthy is the N-terminal part, which is known to contain a lipid binding site and which is involved in trimerization.[13,14] The LHCII structure is not only important for the study of LHCII itself, it also serves as a model for the structure of the minor Chl *a/b* binding proteins CP29, CP26 and CP24 of PSII, the LHCI complexes of photosystem I, early-light induced proteins (ELIPs) and Chl *a/c* binding proteins of Chl *c* containing algae, which all share a large amount of sequence homology with LHCII.[3,15,16]

In view of the light-harvesting function, the pigments are of particular interest. The model shows 12 chlorophylls (Chls), two central carotenoids (xanthophylls or Xans) plus the added neoxanthin. The two central xanthophylls that were originally resolved in the structure were found to have an important structural role and were attributed to lutein (Lut), because the other xanthophylls, violaxanthin (Vio) and neoxanthin (Neo) were present in substoichiometric amounts in the crystallization mixture. The identity of the Chls (Chl *a* or Chl *b*) could not be resolved from the structural data. The seven Chls, closest to the two resolved Xans, were tentatively attributed to Chl *a* (see below) and they are bound at the binding sites indicated by A1, A2, ..., A7 in Figure 3. Since the appearance of the structure, a multitude of studies have been performed on LHCII and among others, a large variety of spectroscopic data have been collected (the absorption spectrum of LHCII at 77 K is given in Figure 4). These spectroscopic measurements, strongly corroborated by recent reconstitution experiments, have shown that the original assignment of the pigment identities was only partially correct (see below). It is important to realize that a detailed understanding of the functioning and spectroscopy of LHCII is complicated by the relatively low resolution of the crystal structure and the strong overlap of many absorption bands. It is the intention of this paper to give an overview of

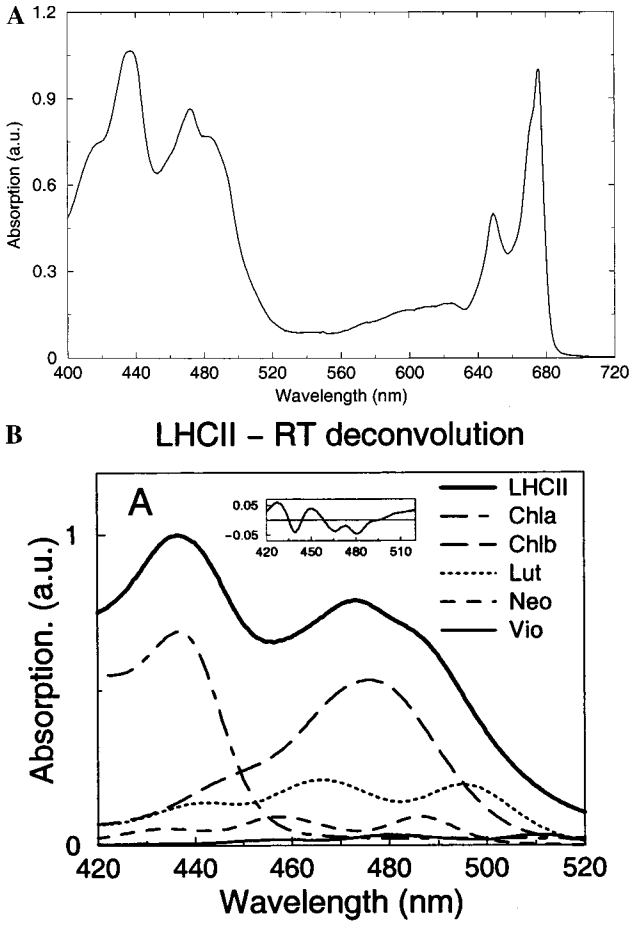

Figure 4. (A) Absorption spectrum of LHCII, recorded at 77 K. Absorption above 670 nm and the peak near 436 nm are mainly due to Chl *a*. Chl *b* peaks near 650 and 460−470 nm. Neo peaks near 486 nm, and Lut and Vio peak above 490 nm. (B) Deconvolution of the absorption spectrum of LHCII at room temperature in the Soret region into the contributions of Chl *a*, Chl *b*, Lut, Neo and Vio. This figure was taken from Gradinaru et al.[74]

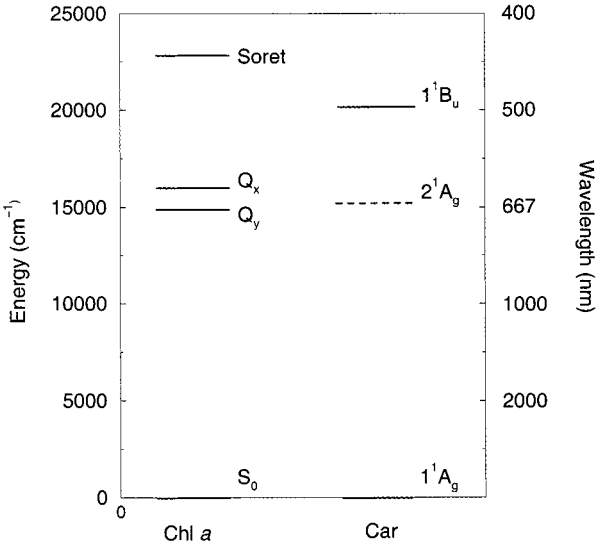

Figure 5. Schematic energy level scheme of Chl *a* and carotenoids (Lut, Vio or Neo). The exact locations of the first excited state of the Cars are not exactly known but they are close to the first excited state of Chl *a*.

TABLE 1: Proposed Chlorophyll Identities at Different Binding Sites in Trimeric LHCII According to Different Studies

site	Kühlbrandt et al.[11]	Remelli et al.[19]	Rogl et al.[20]	Yang et al.[21]
A1	a	a	a	
A2	a	a	a	
A3	a	mixed	a	mixed
A4	a	a		
A5	a	a		
A6	a	mixed or b		
A7	a	mixed or b		
B1	b	a		
B2	b	b		
B3	b	mixed	a	mixed?
B5	b	b	b	
B6	b	b	b	b

the spectroscopic and biochemical experiments with the aim to present a consistent picture. It is, for instance, interesting to compare the properties of LHCII with light-harvesting complexes LH1 and LH2 of purple bacteria. Since the pigment density in the latter complexes is severalfold lower than in LHCII, one might expect that the pigment−pigment interactions in LHCII are much stronger. The reverse appears to be the case. It will become clear that considerable progress has been made since the crystal structure was published and that several important functional properties of LHCII can be understood. On the other hand, many questions remain and a lot of work still has to be done to solve the complicated but rich puzzle, called LHCII.

Chl *a*−*b* Assignment

In the crystal structure of LHCII, 12 chlorophylls were observed per monomeric subunit whereas the LHCII from which the crystals were grown contained 8 Chl *a* and 6 Chl *b* molecules.[11] Seven Chls appeared to be in close contact with the central xanthophylls (Xans) and they were tentatively assigned to Chl *a*, the remaining ones to Chl *b* for the following reason: After rapid downhill energy transfer from Xan and Chl *b* to Chl *a*, a finite probability exists that triplet states are formed on Chl *a* which may lead to the formation of highly reactive singlet oxygen (a schematic energy level diagram is given in Figure 5). In LHCII efficient triplet transfer from Chl *a* to Xan occurs that prevents singlet oxygen formation to a large extent, and which requires close proximity of Chl *a* and Xan (van der Waals contact). Since the publication of the crystal structure, a large number of studies have been performed and it was concluded in several papers that the results of ultrafast spectroscopic experiments and polarized steady-state experiments, but also results from reconstitution experiments, could not consistently be explained with this Chl assignment.[17−21]

Recently, three research groups have addressed the Chl identities by mutating Chl binding sites.[19,20,21] The apoprotein of LHCII was overexpressed in *E. coli*, which allowed the selective mutation of amino acids, in particular those known to bind Chls. LHCII was reconstituted in vitro after mixing the purified apoprotein with a solution containing Chls and Xans. By comparing the spectral properties and pigment composition of LHCII with and without altered binding sites, chlorophyll identities were assigned (see Table 1). Despite some discrepancies between the different studies an improved picture has emerged. We first present the results of Bassi and co-workers[19] who addressed the identities of all 12 Chls. It was concluded that Chls a1, a2, a4 and a5 at binding sites A1, A2, A4 and A5 (see numbering in Figure 3), respectively, are all Chls *a* and Chls b2, b5 and b6 are Chls *b*, in agreement with the original assignment.[11] It was concluded that both sites A3 and B3 each bind on average 0.5 Chl *a* and 0.5 Chl *b* and therefore these

sites are referred to as mixed binding sites. Sites A6 and A7 together bind on average 1.5 Chl *b* and 0.5 Chl *a*. Finally, site B1 was proposed to bind a Chl *a* molecule.[19] Rogl and Kühlbrandt obtained similar conclusions regarding the identities of Chls a1, a2, b5 and b6.[20] In contrast to Bassi and co-workers[19] they concluded that both Chls a3 and b3 are Chls *a* but the data of Rogl and Kühlbrandt were interpreted without allowing for the possibility of mixed binding sites. Yang et al.[21] found that mutation of site A3 led to the loss of ~0.5 Chl *a* and ~0.5 Chl *b*, in agreement with the conclusion by Remelli et al.[5] Mutating site B3 led to the loss of ~1 Chl *a* and ~1 Chl *b*, possibly the Chls at sites B3 and A3. Furthermore, the results from Yang et al. strongly suggest that site B6 binds a Chl *b*, in agreement with the results from the other groups.

Bassi and co-workers also studied the identity of the Chls in CP29 using a similar approach.[22] CP29 binds 6 Chl *a* and 2 Chl *b* molecules and it shows strong sequence homology with LHCII, both in the 3 transmembrane helices A−C and in helix D (40−50% identity). Six of the Chl binding sites that were identified in LHCII are identical for CP29. Moreover, site B6 is a Gln in LHCII and a Glu in CP29 whereas site A2 is an Asn in LHCII and a His in CP29, all potential chlorophyll-binding ligands. These 8 sites appear to bind the 8 Chls in CP29. It was concluded from the mutation study that sites A1, A2, A4 and A5 bind Chl *a*, as in LHCII, whereas sites A3, B3, B5 and B6 are mixed sites. A significant decrease of the Chl *a* to Chl *b* ratio in the reconstitution mixture can lead to a decrease of the Chl *a* to Chl *b* ratio in the complex, whereas the opposite is not possible; i.e., a significant increase of the Chl *a* to Chl *b* ratio with respect to that in vivo has not been observed.[23] Similar results were obtained for LHCII, although the presence of at least one Chl *a* molecule per trimer appeared to be required for the formation of stable trimeric LHCII.[24]

In conclusion, although the identities of the Chls have not been determined with absolute certainty, the proposal by Remelli et al.[19] can also to a large extent explain the results that were obtained for reconstituted LHCII by Yang et al.[20] and Rogl and Kühlbrandt.[21] Furthermore, they are largely consistent with the chlorophyll identities, proposed for CP29[22] in most cases. Below we will use the proposal by Remelli et al. as a working model to address the spectroscopic properties of LHCII. To illustrate the effect of pigment−pigment and pigment−protein interactions in LHCII, we have selected one realization of the pigment identities out of several combinations that are possible in light of the mixed binding sites: Chls *a* are put at sites A1, A2, A3, A4, A5, A7 and B1 and Chls *b* at the remaining sites. This is close to the assignment by Gradinaru et al.[18] based on ultrafast and dichroic measurements, the only difference being that site B5 instead of B1 was assumed to bind a Chl *a* in that study. The orientations of the transition dipole moments cannot be obtained from the crystal structure. By assuming that they are oriented along one of the diagonals of the modeled tetrapyrroles, a most likely orientation was obtained for most of the pigments[18] and these are indicated in Figure 3. The orientations are "0" for all pigments except the one bound at position B3 which has orientation "1" (nomenclature as used by Gülen et al.,[25] i.e., "0" means along NA-NC and "1" along NB−ND). Although this is only one possible configuration (and not necessarily one that occurs in native LHCII) it will be shown that it can account for many experimental observations and therefore, we take it as a reasonable working model.

Chlorophyll−Chlorophyll Interactions in LHCII

Using the transition dipole moment orientations and pigment identities as discussed in the previous section, we can now estimate the coupling strengths between the different chlorophylls. We consider dipole−dipole coupling in the point-dipole approximation. Although this is only approximately correct, it should provide reasonable estimates for most of the interactions and given the uncertainty in the pigment orientations, higher-order approximations would be irrelevant at this stage. The coupling strength V (in cm^{-1}) between two Chl *a* molecules is given by[26,27]

$$V_{12} = \frac{f_l^2 \mu^2}{\epsilon_r} \cdot \frac{5.04\kappa}{R^3}$$

where μ is the transition dipole moment, R is the distance between the centers of the pigments (nm) and the expression for the orientation factor κ is $\kappa = \hat{\mu}_1 \cdot \hat{\mu}_2 - 3(\hat{\mu}_1 \cdot \hat{r}_{12})(\hat{\mu}_2 \cdot \hat{r}_{12})$, where $\hat{\mu}_1$ and $\hat{\mu}_2$ are the normalized transition dipole moment vectors and $\hat{r}_{12}$ is the normalized vector between the centers of pigments **1** and **2**. ϵ_r is the relative dielectric constant and f_l is the local field correction factor. For Chl *b*, the size of μ is 0.84 times that of Chl *a*. In the case of Chl *a*−Chl *b* coupling, μ^2 should be replaced by $|\mu(Chla)||\mu(Chlb)|$.

First we address the values of ϵ_r and f_l, which both depend on the refractive index *n*. It was concluded by Gruszecki et al.[28] from the positions of the S_2 absorption maxima of lutein and neoxanthin that are bound in the interior of LHCII, that the refractive index of their immediate environment is 1.54. Note that the Xan absorption maxima shift linearly with the polarizability of the environment. Furthermore, a value of 1.55 was used by Gradinaru et al.[18] to explain the range of observed excitation energy transfer times and values ranging from 1.47 to 1.55 were needed by Trinkunas et al.[17] in their modeling of the energy transfer in LHCII. Using the cavity-field expression for f_l,[2,29] $(f_l^2\mu^2)/\epsilon_r$ for Chl *a* is calculated to be 17.6 D^2 in the case of $n = 1.55$ and 18.9 D^2 in the case of $n = 1.47$ ($n^2 = \epsilon_r$). Given the fact that the dipole strength for Chl *b* is approximately 30% lower than that of Chl *a*,[30] we arrive at the following approximations for the coupling strength in the case of Chl *a*−Chl *a* (V_{aa}), Chl *a*−Chl *b* (V_{ab}), and Chl *b*−Chl *b* (V_{bb}) coupling, respectively: $(90\kappa)/R^3$, $(75\kappa)/R^3$, and $(63\kappa)/R^3$ (we have taken $n = 1.55$). The resulting interaction Hamiltonian is given in Table 2.

Note that different results are obtained when using the values of the dipole strength that were given by Shipman,[31] where instead of the cavity-field expression, the Lorentz expression was used for the local-field correction. As was recently shown by Alden et al.,[29] the latter correction is not applicable for BChl *a* in different solvents, whereas the former is consistent with absorption measurements. From Table 2 it follows that strong coupling occurs mainly between Chl *a*−Chl *b* pairs, the only exception being the Chl *a*−Chl *a* pair at sites A1 and B1. All other couplings are significantly smaller, well below the width of the absorption bands, which is of relevance for the description of the excited-state energy transfer (see below).

Homogeneous and Inhomogeneous Broadening and (De)localization of Excitations

Several studies have addressed the issue of line broadening in the Q_y region, which is important for understanding both the steady-state spectroscopy and the excitation energy transfer. There are several factors that contribute to the width of the absorption bands. Different binding sites can lead to differences of the absorption maxima (heterogeneity). Also excitonic interactions lead to variations in peak positions. Both effects are generally reflected in polarized spectroscopic properties; i.e.,

TABLE 2: Calculated Dipole−Dipole Coupling Strengths (cm^{-1}) Using the Point-Dipole Approximation for the Q_y Transitions of the Chls at the Indicated Chl Binding Sites[a]

	A1	A2	A3	A4	A5	A7	B1	A6	B2	B3	B5	B6
A1		**40.3**	−2.0	−5.2	12.3	4.5	**86.8**	9.0	−20.0	3.1	2.9	0.4
A2	**40.3**		−2.1	17.2	1.4	−0.6	0.2	16.5	**121.6**	4.3	1.8	−2.8
A3	−2.0	−2.1		−8.3	−17.4	−6.3	2.9	0.7	7.0	**111.9**	2.8	4.8
A4	−5.2	17.2	−8.3		**37.3**	0.7	−8.4	−0.4	5.3	2.3	−20.3	−6.8
A5	12.3	1.4	−17.4	**37.3**		21.5	7.8	1.4	−4.9	1.7	**102.4**	3.8
A7	4.5	−0.6	−6.3	0.7	21.5		−7.4	31.6	−1.2	2.3	−20.5	**67.7**
B1	**86.8**	0.2	2.9	−8.4	7.8	−7.4		−1.4	3.4	−0.1	**51.6**	5.1
A6	9.0	16.5	0.7	−0.4	1.4	31.6	−1.4		−3.7	2.4	−5.7	−23.8
B2	−20.0	**121.6**	7.0	5.3	−4.9	−1.2	3.4	−3.7		−6.4	2.0	2.6
B3	3.1	4.3	**111.9**	2.3	1.7	2.3	−0.1	2.4	−6.4		0.4	−0.8
B5	2.9	1.8	2.8	−20.3	**102.4**	−20.5	**51.6**	−5.7	2.0	0.4		−25.2
B6	0.4	−2.8	4.8	−6.8	3.8	**67.7**	5.1	−23.8	2.6	−0.8	−25.2	

[a] The interactions in the upper left block are between Chl *a* molecules assumed to be present at the indicated sites. The lower right block presents interactions between Chl *b* molecules. Coupling strengths that are larger than 35 cm^{-1} (absolute size) are indicated in bold. For details about the transition dipole moment orientations and the calculation of the coupling, see text.

different transitions contribute to various extents to, for instance, linear and circular dichroism.[32,33] Variations in the environment of a pigment at a particular binding site lead to inhomogeneous broadening.[34] Coupling of the electronic transitions to vibrations of the pigments and of the protein environment (phonons) lead to homogeneous broadening. In an early study by Reddy et al.[34] it was shown that at 4.2 K narrow holes could be burnt near 680 nm in the red wing of the main 676 nm band and it was concluded that the lowest energy state in LHCII peaks near 680 nm with an inhomogeneous width of 120 cm^{-1}.

In fluorescence line narrowing (FLN) measurements at 4.2 K[35] it was observed that fluorescence arises from at least two different Chl *a* molecules because the spectra showed vibronic C═O stretch modes of the 13^1-keto group at 1673 cm^{-1} (Chl *a* which is hydrogen-bonded to the protein) and at 1645 cm^{-1} (different Chl *a* molecule with a very strong hydrogen bond). A recent study on CP29 could even resolve the contributions from three different Chls *a* to the emission spectrum at 4.2 K.[36] These results can be explained in two different ways: (1) the lowest excited state has an excitonic character and the excitation is delocalized over several pigments, or (2) due to inhomogeneity of the site energies of individual pigments, chromophores at different binding sites can have the lowest excited-state energy, due to stochastic variation.

It was reported by Krawczyk et al. that Stark spectroscopy strongly indicates that the states that absorb above 670 nm are essentially localized on individual molecules,[37] which disfavors the first explanation (see also below). In line with these results, Peterman et al.[35] simulated the temperature-dependent shape of the main Q_y absorption band. This band accounts for more than 50% of the Q_y Chl *a* absorption in LHCII, and its intensity corresponds to ∼12 Chls per trimer. The shape of the phonon wing (PW) was estimated from the FLN spectrum at 4.2 K. This simulation approach is based on linear, harmonic Franck−Condon electron−phonon coupling and in this approach the homogeneous broadening (due to electron−phonon coupling) is responsible for the temperature-dependent broadening, whereas the inhomogeneous width is assumed to be temperature-independent. The absorption could be described very well between 4 and 220 K with an inhomogeneous width of 120 ± 15 cm^{-1} (fwhm) and a Huang−Rhys factor of 0.6 ± 0.1 at 4 K for the 12 Chls. Above 220 K the 670 nm band starts to overlap with the 676 nm band to a large extent and, moreover, a weaker band above 680 nm starts to contribute significantly to the absorption above 676 nm[38] and as a consequence the simulations fail.

Making use of the estimated PW, the inhomogeneous width of 120 cm^{-1} and the Huang−Rhys factor of 0.6, Peterman et al. calculated the expected low-temperature (∼4 K) hole-burning spectrum and fluorescence spectrum, assuming that in each individual LHCII, excitations move rapidly to the lowest excited state and that this lowest state is responsible for hole burning and fluorescence.[35] In these simulations all 12 pigments are assumed to have the same average excited-state energy (corresponding to 676 nm) and the same inhomogeneous width, and consequently, they all have an equal probability to possess the lowest excited-state energy. This lowest excited-state energy is stochastically determined and the width of the lowest state is simply governed by the distribution of lowest states in the total ensemble. Applying the above model, it was calculated that the negative peak of the hole-burning spectrum would be located at 679.4 nm and the width would be 72 cm^{-1}, if only the lowest state of the LHCII complexes would be burnt.[35] It can easily be calculated that this width would still be as small as 85 cm^{-1} in the case of only four equivalent and well connected pigments (results not shown). This latter situation would arise in case no energy transfer between the monomeric subunits takes place at 4 K, and it was, for instance, shown by Savikhin et al. that energy transfer is much less efficient at 4 K than at RT (see also below).[39] The calculated width of 85 (or 72) cm^{-1} is substantially smaller than the width of 120 cm^{-1} reported by Reddy et al.[34] However, more recently it was concluded from an extensive hole-burning study that the lowest state is centered around 679.7 nm and has a width of 70 cm^{-1},[40] rather close to the simulated values obtained by Peterman et al.[35]

The position of the lowest state (whatever its exact origin may be) can nicely explain the position of the fluorescence maximum at 680.4 nm. The energy difference with the lowest state at 679.8 (13 cm^{-1}) agrees with the value of the product of the Huang−Rhys factor and the position of the maximum of the PW with respect to the position of the zero-phonon line ($0.8 \times 18 = 14$ cm^{-1},[40] $0.6 \times 22 = 13$ cm^{-1}).[35] If most of the fluorescence arises from the 679.8 nm state, as argued by Pieper et al.,[40] then one might expect that this state will be burnt most efficiently in hole-burning experiments. However, Pieper et al. concluded from their data that the ZPLs of two additional states, centered around 678.4 and 677.1 nm are burnt as efficiently as those of the 679.8 nm state. We are not aware of a good explanation for this apparent discrepancy.

Although the 676 nm band can in zero-order approximation be described by a pool of Chl *a* pigments with the same absorption maximum and the same amount of broadening, one

can definitely not explain all spectroscopic observations perfectly. It was shown that variations of the pigment properties can lead to an improved description of the experimental results.[35] Also the work of Remelli et al.[19] indicates that different pigments contribute to different extents to the main absorption band (but see below). Notwithstanding the fact that the average individual site energies for the Chls, contributing to the 676 nm band, will most likely differ, the statement that the inhomogeneous spread in site energies competes with, and even beats, the spread in average site energies in most of the cases remains valid. In addition, we note that also the strongest coupling strength between Chl *a* pigments (see Table 2) is smaller than the inhomogeneous spread of 120 cm^{-1}. At cryogenic temperatures the inhomogeneous width is much larger than the homogeneous width.[35] Zucchelli et al. studied the absorption thermal broadening of LHCII, and they concluded that the Chl *a* Q_y absorption in LHCII can be described by five absorption bands, all having a width of 210−220 cm^{-1} at room temperature[38] (although the presence of additional substructure can be revealed with other spectroscopic techniques).[32,33,37,41] The contribution of the homogeneous broadening to this width is of a similar order of magnitude as, and even larger than that of the inhomogeneous broadening, in agreement with the results of Peterman et al. for the 676 nm band.[35] A more sophisticated method to describe and fit the temperature dependence of the absorption of LHCII (at 40, 80, and 120 K) was applied by Renger and May.[42] A reasonably good description could be obtained for different assignments of the pigment identities. Using the calculated circular-dichroism spectra to discrimate between these different assignments, they obtain an inhomogeneous width of 140 cm^{-1} with a width of 85 cm^{-1} for the lowest exciton state (calculations for monomeric LHCII), which is located at 680 nm. The Huang−Rhys factor is 0.8. It is not clear how unique the fits are, but the overall resemblance with the above given values is clear.

Monte Carlo Simulations of the (Polarized) Absorption

We have performed Monte Carlo simulations in order to simulate the influence of the exciton coupling and the broadening on the absorption characteristics of LHCII in the Q_y region. The method has, for instance, been described by Kleima et al.[26] In short, to each pigment an (average) excited-state energy is assigned and to model the inhomogeneous broadening, this energy is allowed to vary at random within a certain distribution around the average value. Here, a Gaussian distribution was assumed and the width (fwhm) was taken to be 160 cm^{-1}. This is somewhat higher than the inhomogeneous width of 120 or 140 cm^{-1} given above and also accounts for some homogeneous broadening. As was shown by Somsen et al.,[43] both types of broadening have a similar influence on the exciton spectra. After the site energies are picked at random from this distribution, the interaction matrix is diagonalized and an absorption or LD stick spectrum is obtained. The procedure is repeated many times, a typical number being 100 000 and simultaneously the distribution of lowest energy states is obtained, which reflects an ensemble-averaged absorption band in the current approximation. Because the interactions between the pigments in different monomeric subunits that are observed in the crystal structure, are very weak, we present only spectra, calculated for monomeric LHCII. At first, all average site energies of Chl *a* were taken at 670 nm and those of Chl *b* at 650 nm. The resulting absorption spectrum is given in Figure 6A, together with the spectrum of the lowest state. There is a slight red shift of the absorption with respect to 670 nm, and a weak shoulder

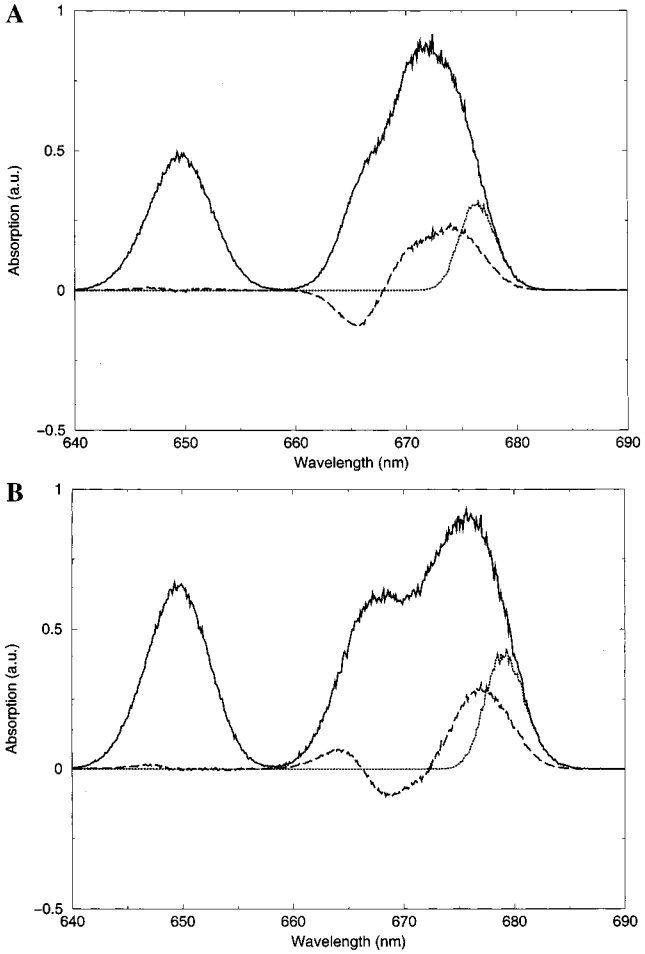

Figure 6. (A) Monte Carlo exciton calculation of different spectra of the LHCII Chls, where the pigment identities and transition dipole moment orientations are taken as indicated in the legend of Figure 2. The site energies of all Chls *a* are taken at 14 925 cm^{-1} (670.0 nm) and those of Chl *b* at 15 385 cm^{-1} (650.0 nm) and an inhomogeneous spread in the site energies of 160 cm^{-1} is taken. Key: solid, absorption spectrum; dashed, LD spectrum; dotted, absorption spectrum of the lowest excited state. For details of the calculation see text. (B) Calculated spectra as in (A), but now the average site energies of the Chls *a* molecules are shifted by −50 cm^{-1} (A1), −100 cm^{-1} (A2), 0 cm^{-1} (A3), −100 cm^{-1} (A4), 0 cm^{-1} (A5), 100 cm^{-1} (A7), and −50 cm^{-1} (B1).

is observed on the blue side of the Chl *a* spectrum. The fwhm of the total Chl *a* band has increased ∼50%, from 160 to 235 cm^{-1}. Because of a variety of excitonic interactions, many different excitonic bands are created and because of the asymmetric pigment organization, they all carry dipole strength, which explains the broadening. In contrast, the width of the Chl *b* band remains almost unaltered, due to the absence of strong Chl *b*−Chl *b* interactions. The intensity of the Chl *a* band has increased by 8% at the expense of intensity in the Chl *b* region. Therefore, the absorption around 650 nm is weaker than one might expect on the basis of the pigment stoichiometry. Ignoring the presence of exciton interactions, the intensity ratio would indicate an apparent Chl *a* to Chl *b* ratio of 1.79 instead of 1.4. It also immediately implies that removing Chls *b* via mutation, can cause a concomitant decrease of absorption in the Chl *a* region, and similar effects are of relevance for the following part of the paper. The simulated spectrum does not account for the vibronic/phonon wing. In reality, the wing of Chl *a* also contributes significantly in the Chl *b* region and its absence explains the fact that the simulated absorption around

TABLE 3: Calculated Förster Transfer Rates (ps^{-1}) from the Chls *b* That Are Assumed To Be Present at the Binding Sites, Indicated in the Left-Most Column[a]

	A1	A2	A3	A4	A5	A7	B1	A6	B2	B3	B5	B6
A6	0.02	0.08				0.29			0.01		0.02	0.36
B2	0.12	4.34	0.01	0.01	0.01		0.01	0.01		0.03		
B3		0.01	3.68						0.03			
B5				0.12	3.08	0.12	0.78	0.02				
B6			0.01	0.01		1.35	0.01	0.36				

[a] For details of the calculation, see text.

660 nm is close to zero, in contrast to what is observed experimentally. However, a perfect description of the absorption spectrum is not our goal here, and we only want to illustrate a few important points.

The lowest-state spectrum peaks at 676.3 nm and it has a width of 85 cm^{-1}. The area of this spectrum is 13.7% of the total Chl *a* absorption band, i.e., close to the area expected for one Chl *a* in the absence of exciton coupling (14.3%). In the absence of coupling the maximum of the lowest-state spectrum is at 674 nm and has a width of 97 cm^{-1} (results not shown). This shows that the exciton coupling does influence the position and width of the lowest state, although the apparent intensity indicates almost complete localization of an excitation on a single Chl *a*. Note that from hole-burning experiments it could also be concluded that the lowest state has the intensity of approximately one Chl *a* (see above). The above simulations show that this does not mean that the excitations are completely localized on a single pigment. After we have discussed the (sub)picosecond time-resolved measurements on LHCII, we will describe simulations with different site energies. Also Renger and May found that delocalization cannot be ignored.[42]

Chlorophyll *b* to Chlorophyll *a* Excitation Energy Transfer

Many studies have addressed the ultrafast excitation energy transfer from Chl *b* to Chl *a* in LHCII. It is now well established that several transfer times coexist as one would expect from the "disordered" pigment arrangement in LHCII.[44−46] It was estimated that at 77 K ~40% of the excitations are transferred with a rate that is faster than $(300\ fs)^{-1}$, ~40% with a rate of $(\sim 600\ fs)^{-1}$ and for ~20% the transfer time is in the range of 4−9 ps.[44] At room temperature the corresponding times depend somewhat on the preparation and they are similar, although the contribution of the fastest component is somewhat larger at the expense of the amount of intermediate component and typical lifetimes are 175 fs, 625 fs, and 5 ps.[45] The approximate average rate is between $(300\ fs)^{-1}$ and $(350\ fs)^{-1}$ in all cases. It was demonstrated by Kleima et al. that the transfer times reflect energy transfer within a monomeric subunit.[46] Agarwal et al. performed three-pulse photon echo peak shift (3PEPS) measurements and found evidence for Chl *b* to Chl *b* energy transfer but the relative amount, when compared to the amount of Chl *b* to Chl *a* transfer, was not determined.[47] The homologous protein CP29 contains on average only 2 Chl *b* molecules, and the observed Chl *b* excited-state lifetimes are 350 fs and 2.2 ps; i.e., they are of the same order of magnitude.[48]

From Table 2 it is clear that the strongest coupling strength within a pair of Chl *b* and Chl *a* molecules is ~120 cm^{-1} which is much smaller than the energetic separation between the Q_y energy levels of the molecules (~450 cm^{-1}). Therefore, the excitonic mixing between the excited states of the molecules is moderate and the excitations are to a large extent localized on either Chl *b* or Chl *a*. This implies that the Förster equation can be applied to estimate the transfer times and it is given by (see, e.g., Förster[49]):

$$W_{DA} = 8.8 \times 10^{17} \frac{k_r^D}{n^4} \cdot \frac{\kappa^2}{R^6} \cdot \int \frac{\epsilon_A(\tilde{\nu})\, f_D(\tilde{\nu})}{\tilde{\nu}^4} d\tilde{\nu} \qquad (8.1)$$

The distance R is expressed in nanometers; the energy is given on a wavenumber scale $\tilde{\nu}$ (given in cm^{-1}). The Förster transfer rate W_{DA} has the same dimensions as the radiative rate k_r^D of the donor molecule. This expression can be written in a shorthanded way as

$$W_{DA} = \frac{C_{DA}}{n^4} \cdot \frac{\kappa^2}{R^6} \qquad (8.2)$$

The following values, which were calculated for room-temperature spectra, were given by Gradinaru et al.[18] $C_{bb} = 14.45$, $C_{ba} = 9.61$ and $C_{aa} = 32.26\ ps^{-1}\cdot nm^6$. (Note that experimental data for excitation energy transfer from Chl *b* to Chl *a*, obtained at RT and 77 K are similar; see above). Using $C_{ba} = 9.61\ ps^{-1}\cdot nm^6$ and taking the Chl assignments and dipole orientations as given before, transfer rates can be calculated if a proper value is chosen for n. Taking $n = 1.55$ (see above), one obtains the results as given in Table 3. This value for the refractive index is also in agreement with the value of $n = 1.6 \pm 0.1$ obtained for the Chl *a* to Chl *a* energy transfer in the peridinin-chlorophyll-*a*-protein.[50]

The calculated rates for energy transfer from the Chls *b* at positions A6, B2, B3, B5 and B6 toward Chl *a* are $(2.6\ ps)^{-1}$, $(223\ fs)^{-1}$, $(270\ fs)^{-1}$, $(243\ fs)^{-1}$ and $(725\ fs)^{-1}$, respectively, relatively close to the experimental rates. The average rate is calculated to be $(355\ fs)^{-1}$. The calculated rates for transfer from Chl *b* to Chl *a* are much larger than those for Chl *b* to Chl *b*, except for the Chl *b* at position A6. The calculated rate of transfer from Chl *b* (A6) toward the Chl *b* at position B6 is 0.36 ps^{-1} (or $(2.8\ ps)^{-1}$) whereas the sum of the rates toward all Chl *a* molecules from Chl *b* (A6) is $(2.6\ ps)^{-1}$. Therefore, this pair of Chls *b* may be responsible for the Chl *b* to Chl *b* transfer that is experimentally observed.[47] One should note that the Chl at position A7 may also be a Chl *b*, in which case it may also contribute to the slow Chl *b* to Chl *a* transfer $(3.5\ ps)^{-1}$ and competing energy transfer between Chl *b* molecules at positions A6, A7 and B6 will take place. Alternatively, if the mixed sites B3 and A3 are both occupied by 2 Chl *b* molecules, equilibration between them on a time scale of hundreds of femtoseconds will precede relatively slow transfer to Chl *a* (see below).

Chlorophyll *a* to Chlorophyll *a* Excitation Energy Transfer

An extensive study of the Chl *a* to Chl *a* transfer kinetics in trimeric LHCII was performed by Visser et al. at 77 K.[44] At this temperature the absorption spectrum shows much more fine structure than at room temperature which allows relatively

TABLE 4: Calculated Förster Transfer Rates (ps^{-1}) from the Chls *a* That Are Assumed To Be Present at the Binding Sites, Indicated in the Left-Most Column[a]

	A1	A2	A3	A4	A5	A7	B1	sum	time
A1		1.12		0.02	0.10	0.01	5.2	6.45	155 fs
A2	1.12			0.20	0.27			1.59	629 fs
A3				0.05	0.21	0.03	0.01	0.29	3.5 ps
A4	0.02	0.20	0.05		0.96		0.05	1.28	780 fs
A5	0.10	0.27	0.21	0.96		0.32	0.04	1.90	526 fs
A7	0.01		0.03		0.32		0.04	0.40	2.5 ps
B1	5.2		0.01	0.05	0.04	0.04		5.34	187 fs

[a] For details of the calculation see text. The column that is headed by "sum" contains the summed transfer rates of the Chl *a* in the same row to all other Chl *a* molecules in the same monomeric subunit. Note that for calculating these sums, the untruncated individual transfer rates have been summed, which may lead to some small differences with summation after truncation. The column that is headed by "time" contains the inverse of the summed transfer rates in the neighboring column. For each element this would reflect the observed single-site lifetime for the Chl in the same row if excitation transfer would be unidirectional from the indicated Chl *a* to all other Chls *a* in the same monomeric subunit.

detailed observations. Thus, it was shown that excitation at 663 nm gives rise to a ~2 ps transfer time, reflecting transfer to pigments absorbing at longer wavelength, whereas excitation around 670 nm leads to transfer steps with time constants of ~400 fs and ~15 ps. More recently, similar experiments were performed by Gradinaru et al.[18] on monomeric LHCII at 77 K. In general, the results were comparable to those observed for trimers but more details were observed. Excitation at 663 nm showed excitation transfer toward longer wavelength pigments with a time constant of 5 ± 1 ps and it was argued that this is due to the transfer originating from only one Chl *a* pigment. After excitation at 669 nm two (downhill) transfer times of 300 fs and 12 ps were observed with similar amplitudes. Upon excitation at 678 nm equilibration processes of several hundreds of femtosecond and of 7−8 ps were found.[18] Thus, it is clear that even within a monomer, besides ultrafast components, also "slow" processes are present, reflecting the structural aymmetry of LHCII. Recent 3PEPS measurements at room temperature revealed Chl *a* equilibration times ranging from 300 fs to 6 ps.[47] It should be noted that energy transfer between two molecules that is almost unidirectional at 77 K may become bidirectional at RT and equilibration between both molecules speeds up. This can to a large extent explain why in the latter study the slowest observed transfer time has approximately half the value of the slowest time at 77 K.

Using the assignment of pigment identities and dipole orientations given above we can now try to relate the experimental observations to model calculations. In Table 4 the calculated transfer rate from every individual Chl *a* to all other Chls *a* in the monomeric subunit is given, using again the Förster equation; most coupling strengths are small, the maximum value of 86.8 cm^{-1} (between Chls at sites A1 and B1) is smaller than the width of the absorption bands. Note that these estimated rates are only approximately correct, since we do not take into account specific site energies and the correct spectral shapes at 77 K. First of all we ask the question which single Chl *a* molecule can be responsible for the Chl *a* peaking near 663 nm and which leads to a transfer time of several picoseconds. From Table 4 it is clear that most Chls transfer relatively rapidly, and only for the Chls at positions A3 and A7 are calculated single site lifetimes of 3.5 and 2.5 ps, respectively.

Considering next the 12−14 ps transfer time, which is observed after excitation near 670 nm, again the Chls at sites A3 and A7 are the only candidates. However, the calculated times are too short. This can only be "repaired" if the Chl at position A5 has a higher or at least similar energy, in which case transfer to this Chl is (partly) blocked. Complete blocking leads to a calculated single-site lifetime of 12.5 ps, when the Chl at A3 peaks near 670 nm, and again 12.5 ps, when the Chl at A7 peaks near 670 nm (note that apparent contradictions with the numbers in Table 4 are entirely due to the fact that truncated values are given for the individual rates). The single site lifetime for the Chl at A5 is then close to 600 fs (i.e., it can either not transfer to the Chl at A3 or to the one at A7), which could explain the fast component (300−400 fs; see above) that is observed upon excitation near 670 nm and which is probably also contaminated with the contribution from some ultrafast vibrational relaxation.

The remaining Chls *a* should be responsible for the main band around 676 nm. According to the calculated rates given in Table 4, equilibration between these Chls should take place on a subpicosecond time scale with the exception of the Chl *a* at position A4, which has a single-site lifetime of many picoseconds, given the fact that transfer to the Chl at position A5 is blocked at 77 K. Qualitatively, the coexistence of subpicosecond and picosecond components for equilibration in the 676 nm band is in agreement with the experimental results.

Again we emphasize that the above realization of the structure represents just one possibility. If, for instance, both Chls at sites B3 and A3 would be Chls *a* (giving rise to absorption around 670 nm), one could also easily explain the slowest observed component of 12−14 ps. One should also keep in mind that there may be an additional Chl *a* molecule, which is not observed in the crystal structure, that could be responsible for the slowest transfer time. Although the Chl at A6 might be a Chl *a*, the transfer would be much faster than 10 ps in that case and thus this Chl cannot be responsible for the slow transfer time.

We have modeled the energy transfer between Chl *a* molecules with the Förster equation, and this is justified for weak coupling, and for the transfer processes that occur on a time scale well above 1 ps. Therefore, the above assignment of the energy levels to the different pigments is justified (A3, A5, A7 are relatively blue, the remaining Chls *a* are responsible for the 676 nm band). The fastest transfer processes correspond to relatively strongly coupled molecules. In that case, significant exciton splitting occurs and relaxation between exciton levels may be a more proper way to describe the dynamics of the corresponding pigments. It was shown by Vulto et al.[51] that the subpicosecond dynamics in the BChl *a* containing Fenna−Matthews−Olson complex can be described by such a relaxation.

Remelli et al. have also addressed the issue of the site energies of different Chls by comparing the absorption spectra of reconstituted LHCII with and without mutated binding sites.[19] Thus, it was concluded that the Chls at positions B1, A1 and A2 contribute to a large extent to the main absorption band on the long-wavelength side, supporting the above assignment that was based on the energy transfer studies. According to Remelli et al.,[19] the Chls at sites A4 and A5 peak near 674 nm and the Chl at site A3 is responsible for an absorption band, peaking near 662−663. This would imply that the Chl bound at site A7 would peak near 670 nm in order to explain the low-temperature peak at this wavelength in the absorption spectrum and the slow transfer component of 12−14 ps. These results are consistent with the above analysis of the Chl *a* to Chl *a* transfer data with one exception: The Chl at position A5 does not peak near 670

nm or below, and therefore, the slowest transfer time (12−14 ps) cannot be explained within the context of the assumed pigment assignment. Although there may be alternative explanations for the slow component (see above), one should also realize that the removal of a Chl at a particular binding site will only lead to an absorption difference spectrum that reflects the absorption spectrum of that particular Chl, if the absorption spectra of the remaining Chls remain unaltered. In the presence of excitonic interactions this is no longer true and this issue will be addressed below.

Energy Transfer between Monomeric Subunits

It was demonstrated by Kleima et al. that all Chl *b* to Chl *a* transfer processes can be assigned to events within a monomeric subunit.[46] Subsequent excited-state equilibration between monomers within a trimer is obtained via Chl *a* to Chl *a* transfer. Instead of addressing this issue by solving an extensive set of differential equations, we will discuss it in a simplified but (hopefully) more illustrative way. Energy transfer from monomer to monomer takes place almost exclusively via the Chls *a* at the central positions A4 and A5 of the trimer and we consider first only these Chls. At RT the transfer from Chl a4 to Chl a5 occurs with a rate of approximately 1 ps^{-1} and the equilibration is twice as fast. Thus, at RT an excitation has equal probability to be located on either Chl. Transfer from Chl a5 to Chls a4 and a5 (a4′ and a5′) in one of the neighboring monomers occurs with rates 0.012 and 0.020 ps^{-1}, respectively, which gives a summed rate of 0.032 ps^{-1}. The rate of transfer from Chl a4 to Chl a4′ is negligible and to Chl a5′ is 0.067 ps^{-1}. Given the fact that the excitation spends approximately equal times on Chls a4 and a5, the average rate is about 0.050 ps^{-1}. Taking into account that we are dealing with a trimer, the equilibration rates between the Chls at all A4 and A5 sites is 3×0.050 ps^{-1} (see van Amerongen and Struve[52] for a similar discussion). On the other hand, if all 7−8 Chls *a* per monomer have comparable energies at RT, this rate should be divided by 3.5−4 (decrease in probability that an excitation resides on Chl a4 or a5), giving a rate of equilibration of 0.038−0.043 ps^{-1}, which corresponds to 23−26 ps. This value will become somewhat larger due to an additional equilibration time within the monomer, and taking the slowest observed spectral equilibration time for LHCII (spectral equilibration already occurs within each of the spectrally almost identical monomers) at room temperature, namely, 6 ps,[47] we arrive at an equilibration time within a trimer of ∼30 ps. It is immediately clear from the above discussion that Chl a5 plays a crucial role in equilibration within the trimer. Taking out this chromophore would dramatically slow the equilibration. This can be mimicked by cooling an LHCII-containing sample to cryogenic temperatures. If Chl a5 absorbs near 670 (as argued above), transfer between monomers via Chl a5 will be thermodynamically very unfavorable. It has indeed been shown by Savikhin et al.[39] that at 13 K equilibration within the trimer is severely hampered: The residual anisotropy for polarized pump−probe measurements increases significantly upon cooling the sample.

One can study transfer throughout the trimer experimentally via singlet−singlet annihilation measurements.[53] In such an experiment, two excitations travel through the trimer until they collide at the same site, creating a higher excited state, that relaxes on a femtosecond time scale by which effectively one of the excitations disappears. The rate of annihilation should be approximately twice as large as the spatial equilibration rate within a trimer for a single excitation, assuming that two excitations lead to immediate annihilation when they meet. The latter assumption may not be entirely justified when the Förster transfer step to an excited Chl *a* molecule is slower than to a Chl *a* in the ground state. This occurs when the excited-state absorption of Chl *a* is smaller than the ground-state absorption in the wavelength region of interest. This is, for instance, the case for bacteriochlorophyll *a*.[54] Barzda et al. obtained an annihilation rate for trimeric LHCII at room temperature of $(24\ ps)^{-1}$.[53] An annihilation time of 28 ps was determined by Bittner et al.[55] The rate of annihilation was also measured for aggregated LHCII, and when the results were corrected to an annihilation rate per trimer, a value of $(16\ ps)^{-1}$ was obtained, faster than for isolated trimers, which is at least partly due to the opening of different transfer routes upon aggregation.[53] A rate of $(16\ ps)^{-1}$ implies that the equilibration time for a single excitation per trimer is $2 \times 16\ ps = 32\ ps$, close to the value, estimated above.

Consequences of Different Binding Sites for the Absorption Spectrum of LHCII

In Figure 6B the absorption spectrum is given that is calculated by assuming different site energies of the pigments and accounting for the exciton coupling. The pigment assignment, dipole orientations and coupling strengths were again taken the same as above. The site energies were chosen to yield spectral equilibration kinetics that are in qualitative agreement with the results from the ultrafast transient absorption measurements as discussed above (see legend of Figure 6B). It is clear that the shape of the absorption spectrum starts to resemble more the experimental spectrum. The simulated Chl *b* absorption band is clearly too narrow, demonstrating that also the Chl *b* molecules have different site energies, but we do not have sufficient information yet to estimate these energies. A perfect description cannot be expected for the absorption spectrum since the effect of mixed binding sites was not accounted for and also the electron−phonon coupling and vibronic contributions were not included.

However, one important aspect of the calculations can easily be illustrated. In Figure 6B the site energies for the Chls at positions A4 and A5 were taken at 674.5 and 670 nm, respectively. The major effect of a mutation of these binding sites is the removal of the corresponding pigment. When the absorption spectra for these "mutants", which are lacking either the Chl at site A4 or A5, are calculated, these are not just the absorption spectrum of the "wild-type" (WT) protein minus the spectrum of the individual Chl, but additional changes occur because of a change in exciton interactions. This is illustrated in the calculated absorption difference spectra in Figure 7. The calculated wildtype-minus-A4 mutant difference spectrum shows a peak near 676 nm, close to the position of the site energy of the Chl at A4 (674.5 nm). However, the wildtype-minus-A5 mutant difference spectrum shows a peak near 675 nm, 5 nm away from the site energy. There is an additional peak present near 665 nm. In the real mutation study,[19] peaks were observed at 674 nm for both mutants, from which it was concluded that the corresponding site energies are also located at these wavelengths. Although the experimental difference spectra differ from our spectra, in the sense that they show additional peaks at different wavelengths, it should be clear that the difference spectra should be interpreted with care. Before drawing any conclusion about site energies, the interaction between all the pigments should be taken into account.

In Figure 6B the calculated LD spectrum is also shown. A major difference with the real LD spectrum is the presence of a negative peak around 670 nm, whereas in the experimental

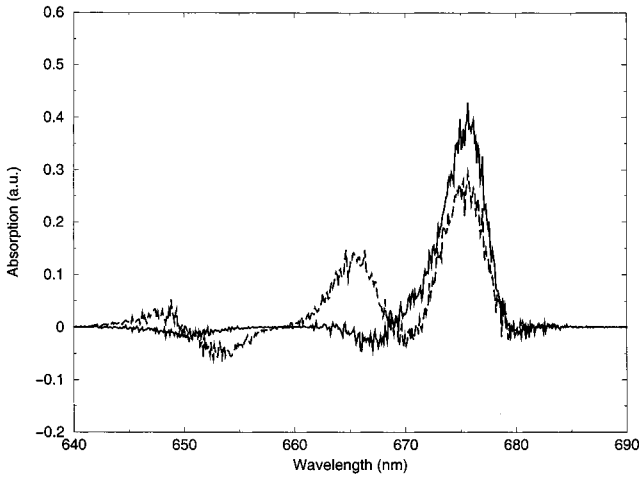

Figure 7. (Solid) absorption difference spectrum. The absorption spectrum, calculated as in Figure 6B, with the Chl at site A4 left out, has been subtracted from the spectrum in Figure 6B. (Dash) absorption difference spectrum. The absorption spectrum, calculated as in Figure 6B, with the Chl at site A5 left out, has been subtracted from the spectrum in Figure 6B.

spectrum the LD is small at this wavelength but not negative.[56,57] However, the positive features near 677 and 664 nm are also present in the experimental spectrum, whereas the LD in the Chl *b* region is small, both for the simulations and the experiment. It should be kept in mind that the exact orientations of the transition dipole moments are not known because the Chls are not defined accurately enough in the crystal structure for precise calculations. However, the global resemblance without optimizing any features, gives hope for an improved resemblance in the future, when, for instance, phonon wings are also taken into account.

The lowest-state spectrum now peaks at 679.0 nm and has a width of 89 cm^{-1}. Its integrated intensity corresponds to 14.2% of the total intensity in the Chl *a* region, similar to the result above. When these percentages are calculated for the other Chl *a* states, they all appear to be between 10.4 and 20.3%.

Xanthophylls in LHCII

LHCII from dark-adapted plants usually contains Lut, Neo and Vio in a ratio of about 2:1:0.07−1, depending on the aggregation state, source and biochemical isolation procedure.[12,58,59,60] This points to a total number of four binding sites per monomeric subunit of a trimer, which now indeed have been recognized. The first two binding sites refer to the Xans resolved in the crystal structure.[11] Both sites can be occupied by Lut and Vio, but with a very strong preference for Lut,[12,61] whereas the binding affinity for Neo is extremely small.[61] The third site was not recognized in the crystal structure. However, it was found by Rogl and Kühlbrandt[20] and by Croce et al.[12] that in reconstituted complexes, where the binding site for either Chl *b*5 or Chl *b*6 was mutated in such a way that no Chl could bind at these positions, 50% less Neo was present, which was taken to imply that the location of Neo is near these two Chl *b* pigments in the vicinity of helix C. Making also use of LD measurements, the location and orientation of Neo was modeled[12] (see Figure 2). The corresponding binding site is highly specific for Neo[12,59] and Hobe et al.[61] found that the affinity for Lut is 25 times lower. The fourth site is probably exclusively occupied by Vio. It was recently shown by Ruban et al.[60] that approximately one Vio is bound per monomeric subunit of LHCII, but the binding is weak and the Xan is very easily lost upon isolation. The Chl *a* molecules are probably located next to the central xanthophylls, whereas one is probably located next to Vio in the fourth position. Evidence for this was given by Peterman et al.[58] who detected an ∼80% efficiency of Chl *a* to Xan triplet transfer in monomeric LHCII (largely depleted of the Xan at the fourth binding site) and a significantly higher efficiency in trimeric LHCII (with partly occupied fourth binding site).[62−64] Gruszecki et al. studied monolayers of LHCII and concluded that Neo and Lut are in an environment with a similar polarizability (refractive index $n = 1.54$) whereas the environment for Vio is entirely different ($n = 1.86$) and it is probably located at the periphery of the complex.[28] It should be noted that the absorption bands of xanthophylls are broad and overlap significantly, and therefore the positions of the maxima are only approximate.

Several reports have suggested that Lut at the first two sites absorb near 494 nm (their red-most absorption peak), whereas Neo at the third binding site absorbs at 486 nm and Vio at the fourth binding site absorbs at 510 nm.[28,58] Various functions have been suggested for the Xans. The central Xans absorbing maximally at 494 nm are probably structurally important.[65] They give rise to very efficient (∼100% at room temperature) singlet energy transfer to Chl.[58] In addition, they accept a large fraction of the Chl *a* triplets.[58,62,63] This means that there must be close contacts between these Xans and at least some Chl *a* residues, in agreement with the Chl assignment given above. As was pointed out above, the triplet quenching is physiologically very important. The Xans quench triplets rather effectively and the rate of transfer was estimated to be $>(0.5\ ns)^{-1}$ by Schödel et al.[66] The energy of the Xan triplets is too low to lead to the formation of singlet oxygen and thus the Xans fulfill a protective role.[67−69] It was concluded by Siefermann-Harms and Angerhofer that the proximity of Chl and Xan is not sufficient to protect the pigments from photooxidation.[67] They proposed that, in addition, an O_2-barrier (provided by the intact structure of LHCII) is required that limits the access of O_2 to the pigment sites. In contrast to the central Xans, the Neo at the third binding position was found to perform badly in singlet excitation energy transfer and triplet quenching.[58] It was found by Croce et al.[59] that reconstituted complexes with Neo suffer less from photooxidation in the presence of oxygen than complexes without Neo and it was proposed that Neo is actively involved in the scavenging of $^1O_2^*$. The Vio at the fourth binding position, absorbing maximally at 510 nm was found to be efficient in singlet energy transfer to Chl, and very efficient in accepting triplets from Chl *a*.[58] Even in complexes with substoichiometric amounts of Vio, a relatively large fraction of the Chl *a* triplets is still transferred to Vio, indicating that it might play an important photophysical role. It was recently determined in our group, with the use of time-resolved fluorescence quenching experiments, that one to two Chl *a* molecules per trimer are not able to transfer triplets to Xan molecules.[64] These Chl *a* molecules are, however, close to the other Chl molecules of LHCII because triplets on these "isolated pigments" are able to quench the singlet excitations located on the other Chls.

Chlorophylls and Xanthophylls in LHCII Influence Their Mutual Spectroscopic Properties

ADMR measurements of van der Vos et al. showed that triplets located on the Xans give rise to absorption changes in the Chl *a* Q_y region between 670 and 680 nm, indicating close contacts between Xan and some Chls *a*, whereas comparable changes for Chl *b* were absent (see also the results of Carbonera

and Giacometti).[71] Similar results were later obtained with flash-induced triplet-minus-singlet (T−S) absorption difference measurements.[58,62,63,72] Excitation in the extreme red edge of the LHCII absorption appeared to lead to a relatively higher yield of triplet transfer toward Lut, with a triplet absorption peak just below 510 nm. Exciting more to the blue led to a relative increase of triplets absorbing around 525 nm, which is ascribed to violaxanthin,[58] indicating preferential contacts between Vio and relatively blue Chls *a*. Also ADMR measurements unveiled a correlation between the red Xan (which is Vio according to Peterman et al.,[58] although at that time van der Vos et al. had a different assignment) and relatively blue Chl *a* molecules.[70] No indication was found for triplets located on the Xan that has its main S_2 absorption band at 486 nm, and which is nowadays ascribed to Neo (see above).

When LHCII is reconstituted without Neo, relatively strong changes are observed in the Chl *b* regions of the absorption, circular dichroism (CD) and LD spectra when compared to native LHCII,[12,59] much stronger than the changes in the Chl *a* region, which is easily understood if most Chls *a* are relatively far away from Neo.

The influence of the Xan triplets on the Chl absorption prompted us to perform the "reversed" experiment, exciting Chls in the Q_y region and probing the Xan absorption region. Indeed, singlet excitation of Chl *a* (at 670 and 680 nm) led to instantaneous (within the time resolution of the experiment, ∼350 fs) spectral changes in the Xan absorption region with negative peaks at 494 nm (Lut) and 510 nm (Vio) whereas excitation of Chl *b* led to a pronounced bleaching at 486 nm (Neo and Chl *b*).[73] The small signals were interpreted as the bleaching of Xan absorption bands superimposed on a broad background due to Chl excited-state absorption. Recently, we have performed similar experiments with substantially lower excitation intensity and the results are very much alike (unpublished results).

Singlet Excitation Energy Transfer from Xanthophylls to Chlorophylls in LHCII

A variety of subpicosecond transient absorption studies has been performed, with the aim to directly observe Xan to Chl energy transfer in LHCII.[74−77] In these studies ultrafast energy transfer to Chls is observed that mainly takes place within several hundreds of femtoseconds. However, contradictory conclusions have been obtained about the identities of the Chls that accept the excitations. In general, the interpretation of the results from these studies is not straightforward, since it is impossible to selectively excite particular Xans, because the absorption spectra of all Xans and Chls *b* show substantial overlap (see Figure 4B). Connelly et al. excited LHCII from *Arabidopsis thaliana* at 475 and 490 nm at room temperature.[76] Upon excitation at 490 nm, only very little immediate bleaching of Chl *b* (<10%) was observed at 652 nm (instrument response time was ∼90 fs). Subsequently a rapid ingrow of the bleaching occurred at this wavelength with a time constant of 142 fs, interpreted as direct energy transfer from Xan to Chl *b*. Direct transfer from Xan to Chl *a* appeared to be absent. A model was presented by these authors in which 2 Chl *b* molecules are positioned close to the central Xans. This specific model conflicts with other results on mutated reconstituted complexes (see above). In addition, the assumption of only a very limited amount of directly excited Chl *b* seems to be in conflict with the occurrence of extensive spectral overlap in the region of excitation.[74,75] In a study by Peterman et al.[75] a substantial amount of direct Chl *b* excitation was indeed observed.[75] In that case excitation at 500 nm (Chl *b* and mainly Lut) showed in addition rapid energy transfer (∼220 fs) from Xan to Chl *a*, characterized by an ingrow of the bleaching and stimulated emission (SE) around 675 nm. In contrast, excitation at 514 nm (Chl *b*, Lut and mainly Vio at the fourth binding position) led to transfer to a Chl *a* spectral form with bleaching/SE around 670 nm. It was argued that only a small fraction of Xan to Chl *b* transfer could have occurred with the time resolution of about 160 fs employed in the experiment. The contacts of both Lut and Vio with Chl *a* molecules having different absorption characteristics is in agreement with T−S results (see above).[70,58] Similarly, from one- and two-photon femtosecond experiments, Walla et al. came to the same conclusion, namely that transfer mainly takes place from Xan to Chl *a*.[77]

Spectral and kinetic information on energy transfer from xanthophylls to chlorophylls within LHCII and CP29 was obtained in a recent femtosecond transient absorption study, by using selective Xan excitation (489, 506 nm) and detecting the induced changes over a wide spectral interval (460−720 nm).[74] It was possible to identify the species (pigments and/or electronic states) which participate in the energy flow, as well as the lifetimes and quantum yields of the individual processes. It was concluded that the initially excited Car S_2 state decays very rapidly, with lifetimes of 70−90 fs in CP29, and 80−120 fs in LHCII, via two competing channels: energy transfer to Chls (60−65%) and internal conversion to the lower, optically forbidden S_1 state (35−40%). In CP29, the energy acceptors are exclusively Chls *a*, while in LHCII this is only valid for lutein and violaxanthin. In LHCII, neoxanthin transfers energy mostly to Chls *b*. In both complexes, ca. 15−20% of the initial Xan excitations are transferred to Chls *a* with a time constant around 1 ps via the S_1 level, thus raising the total Car−Chl transfer efficiency to ca. 80−85%. From the measured transfer rates it was estimated that a coupling of 280−330 cm^{-1} drives the transfer via the S_2 route toward Chls a1, a2, a4 and a5, while a value around 100 cm^{-1} was estimated for the S_1 transfer (in both cases this refers to the sum of couplings).

Mixing of Excited States of Xanthophyll and Chlorophyll Can Shorten the LHCII Excited-State Lifetime

The excited-state lifetime of Chl in trimeric LHCII is shorter than that of Chl in solution (3.5 ns vs 5.5 ns).[78] It has been hypothesized by Razi Naqvi that due to interactions between Chl and Xan, enhanced internal conversion may occur (see, e.g., ref 79 and references therein). Upon aggregation of LHCII, a distribution of lifetimes occurs, a significant part of which is in the order of many hundreds of picoseconds due to the presence of quenchers, the nature of which is still under debate.[53,64,78] In light of the discussion below it is of interest to mention that Ruban et al.[80] showed that a fraction of the Xans in LHCII undergo a trans−cis isomerization upon oligomerization. In the presence of excess light, additional quenchers are created,[81] which lead to an increase of the amount of short excited-state lifetimes.[64] Gruszecki et al.[82] hypothesize that this is partly due to cis−trans isomerization of some Vio. However, Barzda et al. found experimental indications that the enhanced quenching is due to quenchers formed via the triplet states of one or two Chls *a* per trimer, which are not in van der Waals contact with xanthophylls.[64]

It has been speculated that both types of quenching may be related to the so-called nonphotochemical quenching (NPQ) in green plants.[83−85] This is a regulation phenomenon which leads to protection against photodamage under high-light conditions by increasing the amount of excited-state quenching. NPQ is

accompanied by the well-known xanthophyll cycle, which occurs upon acidification of the lumen and during which violaxanthin is de-epoxidated via antheraxanthin to zeaxanthin (Zea).[86] It is still an open question how this cycle is related to NPQ. Two mechanisms have been proposed. The first one is an indirect effect where Zea leads to enhanced aggregation of LHCII, which is accompanied by an increase in the amount of quenching (see above).[84,85] According to the second explanation, direct quenching occurs via the S_1 state of Zea, which was proposed to be lower in energy than the Q_y state of Chl *a*, whereas the S_1 state of Vio was thought to be higher in energy, thereby being unable to function as a quencher.[87] Polivka et al.[88] concluded from femtosecond experiments, probing $S_1 \rightarrow S_2$ transitions, that the S_1 states of both Vio (14470 cm^{-1}) and Zea (14030 cm^{-1}) are lower in energy than the Q_y state of Chl *a*, thereby arguing against such a mechanism. More recently, Frank et al.[89] concluded from steady-state fluorescence experiments, after deconvoluting the contributions from the S_2 and the S_1 state, that the S_1 energy level of Vio is $\sim$14 880 cm^{-1} (672 nm) and that of Zea is $\sim$14 550 cm^{-1} (687 nm). In a subpicosecond two-photon fluorescence excitation study, Walla et al.[77] were able to excite Xans in LHCII via the S_1 state, which led to energy transfer toward Chl *a* and by probing the Chl *a* fluorescence the profile of the involved S_1 state was determined. The estimated 0−0 transition was assumed to be at 653 nm, but it was not entirely clear which Xan would be responsible for it. Therefore, we conclude that still considerable uncertainty exists about the actual S_1-levels in LHCII.

It may be clear from the above discussion that a lot of questions are unanswered, concerning the influence of Xan-Chl interactions on the excited-state lifetime. Below we illustrate via straightforward calculations that the coupling of the Xan S_1 state to the Chl Q_y state may lead to minor changes in the steady-state spectroscopic properties but to significant shortening of the excited-state lifetimes of the Chls, even if the S_1 state is significantly higher in energy than the Q_y state. Although this effect is most likely not responsible for all of the above-mentioned experimental observations, it would on the other hand be very unlikely that it would not contribute to any of the observations, given the approximate knowledge that is available about the energy levels and the coupling strengths.

For illustration of the effect we use the simplest approximation, where the Xan S_1 state and the Chl Q_y state are coupled (all other states are neglected) with coupling strength V_{12}. In the absence of coupling, the Q_y state is assumed to be lower in energy than the S_1 state by an amount δ, the average of their "transition" energies is put at 0 for computational convenience. First-order perturbation theory then leads to two new energy levels: $E^{a,b} = \pm V_{12}\sqrt{1+\Delta^2}$ where $\Delta = \delta/(2V_{12})$ (see, for instance, van Amerongen et al.).[2] The corresponding eigenfunctions are linear combinations of the form $c_{a1}Chl^1Xan^0 + c_{a2}Chl^0Xan^1$ and $c_{b1}Chl^1Xan^0 + c_{b2}Chl^0Xan^1$ and they are delocalized to some extent over both the Chl and the Xan molecule. The superscripts indicate whether a molecule is in the ground (0) or excited state (1). We consider weak interactions, i.e., $V_{12} \ll \delta$, in which case one gets $E^{a,b} = \pm\delta/2(1 + 2V_{12}^2/\delta^2)$; i.e., the energies of the two delocalized states are only slightly repelled with respect to each other when compared to the case of uncoupled chromophores. The probability to find the excitation on either one of the molecules is easily calculated to be V_{12}^2/δ^2 and $1 - V_{12}^2/\delta^2$. This means that the Chl Q_y state is not a pure eigenstate of the system but a small amount of S_1 state is mixed in, the extent of which depends entirely on the value of Δ. The reverse will also happen; i.e., a small amount of Chl Q_y state is mixed into the S_1 state. The dipole strength will hardly change and in (polarized) absorption spectra it will be impossible to observe these effects. The excited-state lifetime of the perturbed S_1 state will hardly be influenced but the excited-state lifetime of the perturbed Chl Q_y state can change to a significant extent. This can be illustrated with the use of some experimental values. The relatively large effect is due to the fact that the excited-state lifetime of Xans is almost 3 orders of magnitude smaller than that of Chl *a* ($\sim$5 ns). The S_1 lifetimes of Vio, Lut and Neo in solution are approximately 24,[88,90] 15,[91,92] and 35 ps.[91] Walla et al.[77] concluded from their two-photon experiments that the 0−0 transition of most of the Xan(s) that transfer(s) excitations via the S_1 state to Chl is located around 15 300 cm^{-1}, meaning that the energy difference δ with the main Q_y band at 676 nm is $\sim$500 cm^{-1}. Gradinaru et al. estimated that the (effective) coupling between the (transferring) S_1 state and the Q_y state is 100 cm^{-1}.[74] In fact, this is an effective coupling of one Xan to two Chls, meaning that the coupling to one Chl is $\sim$70 cm^{-1}, assuming equal coupling for both. Thus, when the Xan−Chl pair is in the lowest excited state, the probability that the excitation is located on the Xan is equal to 0.02. The decay rate from the excited state is thus approximately given by $0.02 \times (0.015\ ns)^{-1} + 0.98 \times (5\ ns)^{-1}$, which corresponds to an excited-state lifetime of $\sim$650 ps. One should realize that the above numbers, as well as the model, provide only rough approximations. However, it should be clear that not only variations in the coupling between Xan and Chl, but also shifts in the energy of the S_1 level (either through isomerization of one of the Xans or the replacement of Vio by Zea and vice versa) can lead to marked changes in the excited-state lifetime of the chlorophylls, even if the S_1 states are significantly higher in energy than the Q_y states.

Comparing LHCII to Other Light-Harvesting Complexes

Although within LHCII ultrafast events occur, on the average the energy transfer in LHCII is relatively slow when compared to a variety of other light-harvesting complexes. It was argued above that spatial equilibration in a trimer, containing 21−24 Chl *a* molecules, takes approximately 30 ps. For instance, excitation of Chl *a* in Photosystem I (PSI) of *Synechocystis sp.* PCC 6803, which contains $\sim$100 Chl *a* molecules, leads to trapping with a time constant of 23−24 ps.[93,94] This time is probably to a large extent determined by relatively slow energy transfer from the antenna pigments to the primary donor.[94] This means that energy transfer between Chl *a* molecules in LHCII occurs on a time scale an order of magnitude slower than in PSI. A qualitative explanation for this difference is the fact that the Chl *a* pigment density is approximately a factor of 2 lower in LHCII as compared to PSI.[11,95] Energy transfer rates that are an order of magnitude larger must correspond to significantly larger coupling strengths between the pigments. It is also of interest to make a comparison with light-harvesting complexes LH2 and LH1 from purple bacteria. For a recent review on the properties of these complexes we refer to the paper of Sundström et al.[96] LH2 and LH1 have ringlike structures with a high degree of symmetry. Both complexes contain BChl *a* molecules as the major pigments, which are responsible for energy transfer to the reaction center. Whereas the absorption maximum of BChl *a* in solution peaks near 770 nm, the absorption peaks of LH2 and LH1 are at 850 and 870 nm, respectively. The enormous red shift is to a significant extent due to strong excitonic interactions. The coupling strength between two neighboring pigments is about 300 cm^{-1} in LH2[97] and probably similar in LH1. These large interactions correspond to extremely fast

equilibration times (several hundreds of femtosecond)[98−101] within the rings of 16−18 (LH2) or 28−32 (LH1) BChls. It should be noted that in plant photosynthesis very strong interactions between Chl molecules would indeed speed up the energy transfer process, but alternatively it would lead to red-shifted energy states. This could reduce the efficiency of light harvesting by LHCII significantly, because the primary donor P680 of PSII has an absorption maximum near 680 nm (i.e., slightly lower in energy than the main excited states in LHCII). This corresponds to the highest energy of all known reaction centers in nature, and this free energy is required to oxidize water. LHCII may have "replaced" several Chls *a* by Chls *b*, which increases the absorption cross-section per amount of protein (which is favorable because protein synthesis is an energetically expensive process) without causing the strong, unfavorable excitonic interactions.

It is argued by Barzda et al.[53] that the effect of the relatively slow transfer in LHCII leads to an increase of the overall trapping time in PSII, which contains on average four LHCII trimers, with ∼120−130 ps (when compared to infinitely fast energy transfer). It is easily calculated that with an excited-state lifetime of ∼3.5 ns of LHCII (in the absence of trapping) this leads to a loss of ∼4% of the excitations due to fluorescence, internal conversion or intersystem crossing, which is not a huge number. For instance, a decrease of quantum efficiency from 99% to 95% may not seem dramatic, on the other hand it may lead to a 5-fold increase of triplet formation on Chl *a*. This can be very harmful for the organism, because of singlet oxygen formation. However, as has been discussed above, the xanthophylls in LHCII are very effective in protecting LHCII against this harmful process, thereby minimizing the potential harmful consequences of "slow" energy transfer.

Conclusions and Outlook

Considerable progress has been made during the last years in characterizing and understanding the spectroscopy and functioning of LHCII. We can qualitatively understand the Chl−Chl and Chl−Xan interactions and the flow of singlet- and triplet transfer. Yet there remains a lot to be done. The issue of the Chl identities has not been settled and the presence of mixed binding sites in vivo should be proven unambiguously. The crystal structure does not reveal all pigments, and the pigment orientations are not known in detail, although the working model that we propose can account for many characteristics. A thorough theoretical understanding of singlet and triplet transfer between Chls and Xans is lacking. Detailed modeling of the spectroscopy, accounting for possible mixed binding sites, exact transition dipole moment orientations, and spectral shapes is clearly a desirable research object for the future. At a higher level of LHCII organization, both in aggregates and in thylakoid membranes, the flow of energy and the involvement in the regulation of energy flow and in nonphotochemcial quenching has to be determined. A thorough understanding of the spectroscopy of LHCII may be of great help for studying the dynamics of protein folding in the case of LHCII.[65] Moreover, it will have significant impact on the understanding of the functioning and spectroscopy of homologous proteins, which are abundant. Finally, it may have some importance for the understanding of evolutionary pathways, which led to the formation of many related proteins, which should have been functional and photostable over billions of years.

Acknowledgment. We thank Drs. R. Croce and R. Bassi for providing Figure 2, which was made by Giuseppe Insana. We thank C. C. Gradinaru for help with the figures and M. Wendling for help with the simulations. Dr. J. P. Dekker is acknowledged for useful discussions.

Note Added in Proof. In a recent study, the small absorption feature at 510 nm was assigned to lutein[102] instead of violaxanthin.[58]

References and Notes

(1) Van Grondelle, R.; Dekker, J. P.; Gillbro, T.; Sundström, V. *Biochim. Biophys. Acta* **1994**, *1187*, 1.
(2) Van Amerongen, H.; Valkunas, L.; van Grondelle, R. *Photosynthetic Excitons*; World Scientific: Singapore, 2000.
(3) Jansson, S. *Biochim. Biophys. Acta* **1994**, *1184*, 1.
(4) Boekema, E. J.; van Roon, H.; Calkoen, F.; Bassi, R.; Dekker, J. P. *Biochemistry* **1999**, *38* 2233.
(5) Boekema, E. J.; van Roon, H.; van Breemen, J. F. L.; Dekker, J. P. *Eur. J. Biochem.* **1999**, *266*, 444.
(6) Boekema, E. J.; van Breemen, J. F. L.; van Roon, H.; Dekker, J. P. *J. Mol. Biol.* **2000**, *301*, 1123.
(7) Dekker, J. P.; van Roon, H.; Boekema, E. J. *FEBS Lett.* **1999**, *449*, 211.
(8) Simidjiev, I.; Barzda, V.; Mustardy, L.; Garab, G. *Anal. Biochem.* **1997**, *250*, 169.
(9) Bassi, R.; Sandona, D.; Croce, R. *Physiol. Plant* **1997**, *100*, 769.
(10) Ruban, A. V.; Philip, D.; Young, A. J.; Horton, P. *Biochemistry* **1997**, *36*, 7855.
(11) Kühlbrandt, W.; Wang, D. N.; Fujiyoshi, Y. *Nature* **1994**, *367*, 614.
(12) Croce, R.; Remelli, R.; Varotto, C.; Breton, J.; Bassi, R. *FEBS Lett.* **1999**, *456*, 1.
(13) Nussberger, S.; Dörr, K.; Wang, D. N.; Kühlbrandt, W. *J. Mol. Biol.* **1993**, *234*, 347.
(14) Hobe, S.; Foster, R.; Klinger, J.; Paulsen, H. *Biochemistry* **1995**, *34*, 10224.
(15) Green, B. R.; Pichersky, E.; Kloppstech, K. *TIBS* **1991**, *16*, 181.
(16) Büchel, C.; Garab, G. J. *Photochem. Photobiol. B: Biology* **1997**, *37*, 118.
(17) Trinkunas, G.; Connelly, J. P.; Müller, M. G.; Valkunas, L.; Holzwarth, A. R. *J. Phys. Chem. B* **1997**, *101*, 7313.
(18) Gradinaru, C. C.; Özdemir, S.; Gülen, D.; van Stokkum, I. H. M.; van Grondelle, R.; van Amerongen, H. *Biophys. J.* **1998**, *75*, 3064.
(19) Remelli, R.; Varotto, C.; Sandona, D.; Croce, R.; Bassi, R. *J. Biol. Chem.* **1999**, *274*, 33510.
(20) Rogl, H.; Kühlbrandt, W. *Biochemistry* **1999**, *38*, 16214.
(21) Yang, C.; Kosemund, K.; Cornet, C.; Paulsen, H. *Biochemistry* **1999**, *38*, 16205.
(22) Bassi, R.; Croce, R.; Cugini, D.; Sandona, D. *Proc. Natl. Acad. Sci. U.S.A.* **1999**, *96*, 10056.
(23) Giuffra, E.; Zucchelli, G.; Sandona, D.; Croce, R.; Cugini, D.; Garlaschi, F. M.; Bassi, R.; Jennings, R. C. *Biochemistry* **1996**, *36*, 12984.
(24) Kleima, F. J.; Hobe, S.; Calkoen, F.; Urbanus, M. L.; Peterman, E. J. G.; van Grondelle, R.; Paulsen, H.; van Amerongen, H. *Biochemistry* **1999**, *38*, 6587.
(25) Gülen, D.; van Grondelle, R.; van Amerongen, H. *J. Phys. Chem. B* **1997**, *101*, 7256.
(26) Kleima, F. J.; Wendling, M.; Hofmann, E.; Peterman, E. J. G.; van Grondelle, R.; van Amerongen, H. *Biochemistry* **2000**, *39*, 5184.
(27) Pullerits, T.; Chachisvilis, M.; Sundström, V. *J. Phys. Chem.* **1996**, *100*, 10787.
(28) Gruszecki, W. I.; Grudzinski, W.; Banaszek-Glos, A.; Matula, M.; Kernen, P.; Krupa, Z.; Sielewiesiuk, J. *Biochim. Biophys. Acta* **1999**, *1412*, 173.
(29) Alden, R. G.; Johnson, E.; Nagarajan, V.; Parson, W. W.; Law, C. J.; Cogdell, R. J. *J. Phys. Chem. B* **1997**, *101*, 4667.
(30) Sauer, K.; Lindsay-Smith, J. R.; Schultz, A. J. *J. Am. Chem. Soc.* **1966**, *88*, 2681.
(31) Shipman, L. L. *Photochem. Photobiol.* **1977**, *26*, 287.
(32) Hemelrijk, P. W.; Kwa, S. L. S.; van Grondelle, R.; Dekker, J. P. *Biochim. Biophys. Acta* **1996**, *1098*, 159.
(33) Nussberger, S.; Dekker, J. P.; Kühlbrandt, W.; van Bolhuis, B. M.; van Grondelle, R.; van Amerongen, H. *Biochemistry* **1994**, *33*, 14775.
(34) Reddy, N. R. S.; van Amerongen, H.; Kwa, S. L. S.; van Grondelle, R.; Small, G. J. *J. Phys. Chem.* **1994**, *98*, 4729.
(35) Peterman, E. J. G.; Pullerits, T.; van Grondelle, R.; van Amerongen. H. *J. Phys. Chem. B* **1997**, *101*, 4448.
(36) Pascal, A.; Peterman, E. J. G.; Gradinaru, C. C.; van Amerongen, H.; van Grondelle, R.; Robert, B. *J. Phys. Chem. B* **2000**, *104*, 9317.

(37) Krawczyk, S.; Krupa, Z.; Maksymiec, W. *Biochim. Biophys. Acta* **1993**, *1143*, 273.
(38) Zucchelli, G.; Garlaschi, F. M.; Jennings, R. C. *Biochemistry* **1996**, *35*, 16247.
(39) Savikhin, S.; van Amerongen, H.; Kwa, S. L. S.; van Grondelle, R.; Struve, W. S. *Biophysical, J.* **1994**, *66*, 1597.
(40) Pieper, J.; Rätsep, M.; Jankowiak, R.; Irrgang, K.-D.; Voigt, J.; Renger, G.; Small, G. J. *J. Phys. Chem. B* **1999**, *103*, 2412.
(41) Kwa, S. L. S.; Groeneveld, F. G.; Dekker: J. P.; van Grondelle, R.; van Amerongen, H.; Lin, S.; Struve, W. S. *Biochim. Biophys. Acta* **1992**, *1101*, 143.
(42) Renger, T.; May, V. *Phys. Rev. Lett.* **2000**, *84*, 5228.
(43) Somsen, O. J. G.; van Grondelle, R.; van Amerongen, H. *Biophys. J.* **1996**, *71*, 1934.
(44) Visser, H. M.; Kleima, F. J.; van Stokkum, I. H. M.; van Grondelle, R.; van Amerongen, H. *Chem. Phys.* **1996**, *210*, 297.
(45) Connelly, J. P.; Müller, M. G.; Hucke, M.; Gatzen, G.; Mullineaux, C. W.; Ruban, A. V.; Horton, P.; Holzwarth, A. R. *J. Phys. Chem. B* **1997**, *101*, 1902.
(46) Kleima, F. J.; Gradinaru, C. C.; Calkoen, F.; van Stokkum, I. H. M.; van Grondelle, R.; van Amerongen, H. *Biochemistry* **1997**, *36*, 15262.
(47) Agarwal, R.; Krueger, B. P.; Scholes, G. D.; Yang, M.; Yom, J.; Mets, L.; Fleming, G. R. *J. Phys. Chem. B* **2000**, *104*, 2908.
(48) Gradinaru, C. C.; Pascal, A. A.; van Mourik, F.; Robert, B.; Horton, P.; van Grondelle, R.; van Amerongen, H. *Biochemistry* **1998**, *37*, 1143.
(49) Förster, Th. In *Modern Quantum Chemistry*; Sinanoglu, O., Ed.; Academic Press: New York, 1965.
(50) Kleima, F. J.; Hofmann, E.; Gobets, B.; van Stokkum, I. H. M.; van Grondelle, R.; Diederichs, K.; van Amerongen, H. *Biophys. J.* **2000**, *78*, 344.
(51) Vulto, S. I. E.; de Baat, M. A.; Neerken, S.; Nowak, F. R.; van Amerongen, H.; Amesz, J.; Aartsma, T. J. *J. Phys. Chem. B* **1999**, *103*, 8153.
(52) Van Amerongen, H.; Struve, W. S. *J. Lumin.* **1992**, *51*, 29.
(53) Barzda, V.; Gulbinas, V.; Kananavicius, R.; van Amerongen, H.; van Grondelle, R.; Valkunas, L. Submitted for publication.
(54) Becker, M.; Nagarajan, V.; Parson, W. W. *J. Am. Chem. Soc.* **1991**, *113*, 6840.
(55) Bittner, T.; Irrgang, K.-D.; Renger, G.; Wasielewski, M. R. *J. Phys. Chem.* **1994**, *98*, 11821.
(56) Van Amerongen, H.; Kwa, S. L. S.; van Bolhuis, B. M.; van Grondelle, R. *Biophys. J.* **1994**, *67*, 837.
(57) Zucchelli, G.; Dainese, P.; Jennings, R. C.; Breton, J.; Garlaschi, F. M.; Bassi, R. *Biochemistry* **1994**, *33*, 8982.
(58) Peterman, E. J. G.; Gradinaru, C. C.; Calkoen, F.; Borst, J. C.; van Grondelle, R.; van Amerongen, H. *Biochemistry* **1997**, *36*, 12208.
(59) Croce, R.; Weiss, S.; Bassi, R. *J. Biol. Chem.* **1999**, *274*, 29613.
(60) Ruban, A. V.; Lee, P. J.; Wentworth, M.; Young, A. J.; Horton, P. *J. Biol. Chem.* **1999**, *274*, 10458.
(61) Hobe, S.; Niemeier, H.; Bender, A.; Paulsen, H. *Eur. J. Biochem.* **2000**, *267*, 616.
(62) Barzda, V.; Peterman, E. J. G.; van Grondelle, R.; van Amerongen, H. *Biochemistry* **1998**, *37*, 546.
(63) Peterman, E. J. G.; Dukker, F. M.; van Grondelle, R.; van Amerongen, H. *Biophys. J.* **1995**, *69*, 2670.
(64) Barzda, V.; Vengris, M.; Valkunas, L.; van Grondelle, R.; van Amerongen, H. *Biochemistry* **2000**, *39*, 10468.
(65) Paulsen, H. *Photochem. Photobiol.* **1995**, *62*, 367.
(66) Schödel, R.; Irrgang, K.-D.; Voigt, J.; Renger, G. *Biophys. J.* **2000**, *75*, 3143.
(67) Siefermann-Harms, D.; Angerhofer, A. *Photosynth. Res.* **2000**, *55*, 83.
(68) Siefermann-Harms, D. *Physiol. Plant* **1987**, *69*, 561.
(69) Nechustai, R.; Thornber, J. P.; Patterson, L. K.; Fessenden, R. W.; Levanon, H. *J. Phys. Chem.* **1988**, *92*, 1165.
(70) Van der Vos, R.; Carbonera, D.; Hoff, A. J. *Appl. Magn. Reson.* **1991**, *2*, 179.
(71) Carbonera, D.; Giacometti, C. G. *Rend. Fis. Acc. Lincei* **1992**, *3*, 361.
(72) Razi Naqvi, K.; Melø, T. B.; Raju, B. B.; Javorfi, T.; Simidjiev, I.; Garab, G. *Spectrochim. Acta A* **1991**, *53*, 2659.
(73) Gradinaru, C. C.; van Stokkum, I. H. M.; van Grondelle, R.; van Amerongen, H. In *Photosynthesis: Mechanisms and Effects*; Garab G., Ed.; Kluwer Academic Publishers: Dordrecht, 1998; p 277.
(74) Gradinaru, C. C.; van Stokkum, I. H. M.; Pascal, A. A.; van Grondelle, R.; van Amerongen, H. *J. Phys. Chem. B*, in press.
(75) Peterman, E. J. G.; Monshouwer, R.; van Stokkum, I. H. M.; van Grondelle, R.; van Amerongen, H. *Chem. Phys. Lett.* **1997**, *264*, 279.
(76) Connelly, J. P.; Müller, M. G.; Bassi, R.; Croce, R.; Holzwarth, A. R. *Biochemistry* **1997**, *36*, 281.
(77) Walla, P. J.; Yom, J.; Krueger, B. P.; Fleming, G. R. *J. Phys. Chem. B* **2000**, *104*, 4799.
(78) Ide, J. P.; Klug, D. R.; Kühlbrandt, W.; Giorgi, L. B.; Porter G. *Biochim. Biophys. Acta* **1987**, *893*, 349.
(79) Razi Naqvi, K. In *Photosynthesis: Mechanisms and Effects*; Garab G., Ed.; Kluwer Academic Publishers: Dordrecht, 1998; p 265.
(80) Ruban, A. V.; Horton, P.; Robert, B. *Biochemistry* **1995**, *34*, 2333.
(81) Jennings, R. C.; Garlaschi, F. M.; Zucchelli, G. *Photosynth. Res.* **1991**, *27*, 57.
(82) Gruszecki, W. I.; Matula, M.; Ko-chi, N.; Koyama, Y.; Krupa, Z. *Biochim. Biophys. Acta* **1997**, *1319*, 267.
(83) Demmig-Adams, B.; Adams, W. W. I. *Annu. Rev. Plant Physiol. Mol. Biol.* **1992**, *43*, 599.
(84) Horton, P.; Ruban, A. V.; Walters, R. G. *Plant Physiol.* **1994**, *106*, 415.
(85) Garab, G. In *Light as Energy Source and Information Carrier in Plant Biology*; Jennings, R., Ed.; NATO/ASI/Plenum Publishing Corp.: New York, 1996.
(86) Demmig-Adams, B. *Biochim. Biophys. Acta* **1990**, *1020*, 1.
(87) Frank, H. A.; Cua, A.; Chynwat, V.; Young, A.; Gosztola, D.; Wasielewski, M. R. *Photosynth. Res.* **1994**, *41*, 389.
(88) Polivka, T.; Herek, J. L.; Zigmantas, D.; Akerlund, H.; Sundström, V. *Proc. Natl. Acad. Sci. U.S.A.* **1999**, *96*, 4914.
(89) Frank, H. A.; Bautista, J. A.; Josue, J. S.; Young, A. J. *Biochemistry* **2000**, *39*, 2831.
(90) Chynwat, V.; Frank, H. A. *Chem. Phys.* **1995**, *194*, 237.
(91) Frank, H. A.; Chynwat, V.; Desamero, R. Z. B.; Farhoosh, R.; Erickson, J.; Bautista, J. P. *Pure Appl. Chem.* **1997**, *69*, 2117.
(92) Frank, H. A.; Bautista, J. P.; Josue, J. J.; Pendon, Z.; Hiller, R.; Sharples, F. P.; Gosztola, D.; Wasielewski, M. R. *J. Phys. Chem. B* **2000**, *104*, 4569.
(93) Savikhin, S.; Xu, W.; Soukoulis, V.; Chitnis, P. R.; Struve, W. S. *Biophys. J.* **1999**, *76*, 3278.
(94) Gobets, B.; van Stokkum, I. H. M.; van Mourik, F.; Rögner, M.; Kruip, J.; Dekker, J. P.; van Grondelle, R. In *Photosynthesis: Mechanisms and Effects*; Garab G, Ed.; Kluwer Academic Publishers: Dordrecht, 1998; p 571.
(95) Krauss, N.; Schubert, W.-D.; Klukas, O.; Fromme, P.; Witt, H. T.; Saenger, W. *Nat. Struct. Biol.* **1996**, *3*, 965.
(96) Sundström, V.; Pullerits, T.; van Grondelle, R. *J. Phys. Chem. B* **1999**, *103*, 2327.
(97) Koolhaas, M. H. C.; Frese, R. N.; Fowler, G. J. S.; Bibby, T. S.; Georgakopoulou, S.; van der Zwan, G.; Hunter, C. N.; van Grondelle, R. *Biochemistry* **1998**, *14*, 4693. Sauer, K.; Cogdell, R. J.; Prince, S. M.; Freer, A. A.; Isaacs, N. W.; Scheer, H. *Photochem. Photobiol.* **1996**, *64*, 564. Monshouwer, R.; Abrahamsson, M.; van Mourik, F.; van Grondelle, R. *J. Phys. Chem. B* **1997**, *101*, 7241. Scholes, G. D.; Fleming, G. R. *J. Phys. Chem. B* **2000**, *104*, 1854.
(98) Chachisvilis, M.; Kühn, O.; Pullerits, T.; Sundström, V. *J. Phys. Chem. B* **1997**, *101*, 7275
(99) Bradforth, S. E.; Jimenez, R.; van Mourik, F.; van Grondelle, R.; Fleming, G. R. *J. Phys. Chem.* **1995**, *99*, 9, 16179.
(100) Visser, H. M.; Somsen, O. J. G.; van Mourik, F.; Lin, S.; van Stokkum, I. H. M.; van Grondelle, R. *Biophys. J.* **1995**, *69*, 1083.
(101) Monshouwer, R.; Baltuska, A.; van Mourik, F.; van Grondelle, R. *J. Phys. Chem. A* **1998**, *102*, 4360.
(102) Ruban, A. V.; Pascal, A. A.; Robert, B. *FEBS Letters* **2000**, *477*, 181.